Inorg. Chem. **2007**, *46*, 6405–6412

Selective Fluorescence Zinc Ion Sensing and Binding Behavior of 4-Methyl-2,6-bis(((phenylmethyl)imino)methyl)phenol: Biological Application

Partha Roy,[†] Koushik Dhara,[†] Mario Manassero,[‡] Jagnyeswar Ratha,[§] and Pradyot Banerjee*,[†]

Department of Inorganic Chemistry, Indian Association for the Cultivation of Science, Jadavpur, Kolkata-700 032, India, Dipartimento di Chimica Strutturale e Stereochimica Inorganica dell'Universitá di Milano, Via G. Venezian 21, 20133 Milano, Italy, and Cellular Biochemistry Division, Indian Institute of Chemical Biology, Jadavpur, Kolkata-700 032, India

Received March 5, 2007

Zinc ion fluorescence sensing and the binding properties of 4-methyl-2,6-bis(((phenylmethyl)imino)methyl)phenol (**HL**) have been investigated. It displays high selectivity for Zn^{2+} and can be used as zinc ion-selective luminescent probe for biological application under physiological conditions. The increase in emission in the presence of Zn^{2+} is accounted for by the formation of hexanuclear complex $[Zn_6(\mathbf{L})_2(OH)_2(CH_3COO)_8]$ characterized by X-ray crystallography. An approximately 6-fold Zn^{2+}-selective chelation-enhanced fluorescence response in HEPES buffer (pH 7.4) is attributed due to the strong coordination of Zn(II) that would impose rigidity and hence decrease the nonradiative decay of the excited state. By incubation of cultured living cells (B16F10 mouse melanoma and A375 human melanoma) with **HL,** intracellular Zn^{2+} concentration could be monitored.

Introduction

Search for reagents which can efficiently act as fluorescence sensors for zinc(II) has been an active area of research.[1−7] The importance of zinc in the biological domain primarily lies in the fact that it is an essential trace element acting as a structural component of proteins and peptides. Its role in the catalytic site of enzymes is also well-known.[8] A topic of substantial current interest, however, stems out of the functionality of zinc in neurobiology.[9] Recent studies have shown that a fraction of Zn^{2+} is found in free or chelatable form in some organs, e.g., brain,[10] pancreas,[11] and spermatozoa.[12] A considerable amount of chelatable Zn^{2+}

* To whom correspondence should be addressed. E-mail: icpb@mahendra.iacs.res.in. Fax: (+91) 33 2473-2805.

† Indian Association for the Cultivation of Science.

‡ Dipartimento di Chimica Strutturale e Stereochimica Inorganica dell'Universitá di Milano.

§ Indian Institute of Chemical Biology.

(1) (a) Liu, Y.; Zhang, N.; Chen, Y.; Wang, L.-H. *Org. Lett.* **2007**, *9*, 315. (b) Nolan, E. M.; Jaworski, J.; Racine, M. E.; Sheng, M.; Lippard, S. J. *Inorg. Chem.* **2006**, *45*, 9748. (c) Mikata, Y.; Wakamatsu, M.; Kawamura, A.; Yamanaka, N.; Yano, S.; Odani, A.; Morihiro, K.; Tamotsu, S. *Inorg. Chem.* **2006**, *45* 9262. (d) Nolan, E. M.; Jaworski, J.; Okamoto, K.-I.; Hayashi, Y.; Sheng, M.; Lippard, S. J. *J. Am. Chem. Soc.* **2005**, *127*, 16812. (e) Nolan, E. M.; Burdette, S. C.; Harvey, J. H.; Hilderbrand, S. A.; Lippard, S. J. *Inorg. Chem.* **2004**, *43*, 2624. (f) Aoki, S.; Kaido, S.; Fujioka, H.; Kimura, E. *Inorg. Chem.* **2003**, *42*, 1023. (g) Koike, T.; Abe, T.; Takahashi, M.; Ohtani, K.; Kimura, E.; Shiro, M. *J. Chem. Soc., Dalton Trans.* **2002**, 1764. (h) Burdette, S. C.; Walkup, G. K.; Spingler, B.; Tsien, R. Y.; Lippard, S. J. *J. Am. Chem. Soc.* **2001**, *123*, 7831. (i) Walkup, G. K.; Burdette, S. C.; Lippard, S. J.; Tsien, R. Y. *J. Am. Chem. Soc.* **2000**, *112*, 5644.

(2) (a) Harrop, T. C.; Mascharak, P. K. *Chemtracts* **2001**, *14*, 442. (b) Kimura, E.; Aoki, S. *BioMetals* **2001**, *14*, 191. (c) Prasanna de Silva, A.; Nimal Gunaratne, H. Q.; Gunnlaugsson, T.; Huxley, A. J. M.; McCoy, C. P.; Rademacher, J. T.; Rice, T. E. *Chem. Rev.* **1997**, *97*, 1515.

(3) (a) Czarnik, A. W. *Acc. Chem. Res.* **1994**, *27*, 302. (b) Akkaya, E. U.; Huston, M. E.; Czarnik, A. W. *J. Am. Chem. Soc.* **1990**, *112*, 3590. (c) Huston, M. E.; Engleman, C.; Czarnik, A. W. *J. Am. Chem. Soc.* **1990**, *112*, 7054.

(4) (a) Kimura, E. *S. Afr. J. Chem.* **1997**, *50*, 240. (b) Kimura, E.; Koike, T. *Chem. Soc. Rev.* **1998**, *27*, 179. (c) Hendrickson, K. M.; Rodopoulos, T.; Pittet, P.-A.; Mahadevan, I.; Lincoln, S. F.; Ward, A. D.; Kurucsev, T.; Duckworth, P. A.; Forbes, I. J.; Zalewski, P. D.; Betts, H. *J. Chem. Soc., Dalton Trans.* **1997**, 3879. (d) Koike, T.; Watanabe, T.; Aoki, S.; Kimura, E.; Shiro, M. *J. Am. Chem. Soc.* **1996**, *118*, 12696. (e) Coyle, P.; Zalewski, P. D.; Philcox, J. C.; Forbes, I. J.; Ward, A. D.; Lincoln, S. F.; Mahadevan, I.; Rofe, A. M. *Biochem. J.* **1994**, *303*, 781. (f) Zalewski, P. D.; Forbes, I. J.; Seamark, R. F.; Borlinghaus, R.; Betts, W. H.; Lincoln, S. F.; Ward, A. D. *Chem. Biol.* **1994**, *1*, 153. (g) Zalewski, P. D.; Forbes, I. J.; Betts, W. H. *Biochem. J.* **1993**, *296*, 403.

(5) (a) Nasir, M. S.; Fahrni, C. J.; Suhy, D. A.; Kolodsick, K. J.; Singer, C. P.; O'Halloran, T. V. *J. Biol. Inorg. Chem.* **1999**, *4*, 775. (b) Fahrni, C. J.; O'Halloran, T. V. *J. Am. Chem. Soc.* **1999**, *121*, 11448. (c) Suhy, D. A.; Simon, K. D.; Linzer, D. I. H.; O'Halloran, T. V. *J. Biol. Chem.* **1999**, *274*, 9183.

(6) (a) Gee, K. R.; Zhou, Z.-L.; Qian, W.-J.; Kennedy, R. *J. Am. Chem. Soc.* **2002**, *124*, 776. (b) Hirano, T.; Kikuchi, K.; Urano, Y.; Higuchi, T.; Nagano, T. *Angew. Chem., Int. Ed.* **2000**, *39*, 1052. (c) Godwin, H. A.; Berg, J. M. *J. Am. Chem. Soc.* **1996**, *118*, 6514.

10.1021/ic700420w CCC: $37.00
Published on Web 07/07/2007

sequestered in the vesicles of presynaptic neurons is released from brain when the neurons become active.[13] However, the effective role of Zn^{2+} is poorly understood with neuronal disorders.[14] An upper limit of estimate ranging to the low millimolar[15] concentration of Zn^{2+} within the neuronal vesicles has been made, and the same in the synapse falls at 10−30 μM.[14,15] Neuronal death can occur owing to uncontrolled Zn^{2+} released from the mossy fiber terminals after traumatic brain injury, stock, or seizure.[16] It is also believed that the Zn^{2+} homeostasis may have some bearing to the pathology of Alzheimer's disease and other neurological problems.[14,17] The lack of appropriate detecting tools for over a quite large concentration range causes a severe hindrance for further investigations of this spectroscopically inaccessible metal ion.

For imaging biological Zn^{2+}, the use of several fluorescent zinc chemisensors is in vogue.[2b,18] The common probes are aryl sulfonamide derivatives of 8-aminoquinoline, such as 6-methoxy-(8-*p*-toluenesulfonamido)quinoline (TSQ)[19] and Zinquin,[4f] as well as Zinbo-5,[20] the Zinpyr (ZP) family,[1h,1i,21−23] and the ZnAF molecules.[24] The water solubility of TSQ poses some problem which has been averted by the introduction of carboxylic acid groups or ester groups to extend the 6-methoxy group[4f,25] and replacement of the methyl group on the benzene ring with a carboxylic acid group substituent.[26] Difficulty arising from the use of such probes lies in their sparing solubility in neutral aqueous solution. Apart from these type of sensors, use of synthetic peptides for signaling zinc is also made which act by the way of fluorescence enhancement.[6c,27] The aryl sulfonamide sensors can in general form 1:1 and 1:2 Zn^{2+}/ligand complexes in such a way that it is possible for a protein-bound zinc ion to activate the change in the dye fluorescence.[18] There are other types of sensors which bind zinc to form either exclusively 1:1 complexes[20,21,24,28] or a mixture of 1:1 and 1:2 species (abbreviated as ZP1 and ZP2).[1h,i] These can impart significant fluorescence changes only when the first Zn^{2+} ion is bound. Although a variety of zinc sensors are reported, there remains much to be done in this aspect. The most powerful approach seems to design small and simple synthetic molecules that combine a Zn^{2+} binding unit with a fluorophore. Significant change in either fluorescence intensity or wavelength on Zn^{2+} coordination occurs making it a suitable analytical tool.

Herein we explore the selective Zn^{2+} sensor property of a simple and small molecule, 4-methyl-2,6-bis(((phenylmethyl)imino)methyl)phenol (**HL**), prepared by Schiff base condensation of 4-methyl-2,6-diformylphenol and phenylmethylamine in HEPES buffer (pH 7.4) at 25 °C. The investigations on the luminescent property in the working buffer show that the emission intensity of **HL** increases significantly upon addition of various concentrations of Zn^{2+}, while the introduction of other transition metal ions and biologically relevant metal ions (Ca^{2+}, Mg^{2+}, Na^{+}, and K^{+}) causes the intensity to be either unchanged or weakened. The system shows selective chelation enhanced fluorescence (CHEF) in the presence of Zn(II) ion. The enhancement of fluorescence is attributed due to the strong binding of Zn(II) evident from a large binding constant value ($1.5 \times 10^4\ M^{-1}$) that would impose rigidity and hence decrease the nonradiative decay of the excited state. The case implies that **HL** could monitor or recognize Zn^{2+} and be considered as a selective luminescent probe. Reaction of zinc(II) acetate and **HL** affords the hexanuclear neutral complex $[Zn_6(L)_2(OH)_2(CH_3COO)_8]$, (**1**) characterized by elemental analysis and single-crystal X-ray structural determination. **HL** exhibits satisfactory Zn^{2+} sensing abilities in the physiological pH range. We have examined the application of the sensor (**HL**) to cultured living cells (B16F10 mouse melanoma and A375 human melanoma) by fluorescence microscopy.

Experimental Section

Materials and Physical Methods. High-purity HEPES and zinc acetate dihydrate were purchased from Sigma Aldrich and were used as received. All other reagents were of analytical grade. Buffer was prepared using deionized and sonicated triple distilled water.

(7) (a) Pearce, D. A.; Jotterand, N.; Carrico, I. S.; Imperiali, B. *J. Am. Chem. Soc.* **2001**, *123*, 5160. (b) Prodi, L.; Montali, M.; Bradshaw, J. D.; Izatt, R. M.; Savage, P. B. *J. Inclusion Phenom. Macrocycl. Chem.* **2001**, *41*, 123. (c) Reany, O.; Gunnlaugsson, T.; Parker, D. *J. Chem. Soc., Chem. Commun.* **2000**, 473. (d) Walkup, G. K.; Imperiali, B. *J. Org. Chem.* **1998**, *63*, 6727. (e) Walkup, G. K.; Imperiali, B. *J. Am. Chem. Soc.* **1997**, *119*, 3443. (f) Fabbrizzi, L.; Licchelli, M.; Pallavicin, P.; Perotti, A.; Taglietti, A.; Sacchi, D. *Chem.—Eur. J.* **1996**, *2*, 75. (g) Walkup, G. K.; Imperiali, B. *J. Am. Chem. Soc.* **1996**, *118*, 3053.

(8) (a) Vallee, B. L.; Falchuk, K. H. *Physiol. Rev.* **1993**, *73*, 79. (b) Berg, J. M.; Shi, Y. G. *Science* **1996**, *271*, 1081.

(9) (a) Vallee, B. L.; Falchuk, K. H. *Physiol. Rev.* **1993**, *73*, 79−118. (b) Frederickson, C. J.; Moncrieff, D. W. *Biol. Signals* **1994**, *3*, 127. (c) Takeda, A. *BioMetals* **2001**, *14*, 343.

(10) (a) Frederickson, C. J. *Int. Rev. Neurobiol.* **1989**, *31*, 145. (b) Frederickson, C. J.; Bush, A. I. *Biometals* **2001**, *14*, 353. (c) Li, Y.; Hough, C.; Sarvey, J. *Sci. STKE* **2003**, *182*, 19.

(11) (a) Zalewski, P. D.; Millard, S. H.; Forbes, I. J.; Kapaniris, O.; Slavotinek, A.; Betts, W. H.; Ward, A. D.; Lincoln, S. F.; Mahadevan, I. *J. Histochem. Cytochem.* **1994**, *42*, 877. (b) Qian, W. J.; Gee, K. R.; Kennedy, R. T. *Anal. Chem.* **2003**, *75*, 3468.

(12) Zalewski, P. D.; Jian, X.; Soon, L. L. L.; Breed, W. G.; Seamark, R. F.; Lincoln, S. F.; Ward, A. D.; Sun, F. Z. *Reprod., Fertil. Dev.* **1996**, *8*, 1097.

(13) (a) Assaf, S. Y.; Chung, S. H. *Nature* **1984**, *308*, 734. (b) Howell, G. A.; Welch, M. G.; Frederickson, C. J. *Nature* **1984**, *308*, 736.

(14) Bush, A. I. *Curr. Opin. Chem. Biol.* **2000**, *4*, 184.

(15) Frederickson, C. J.; Bush, A. I. *Biometals* **2001**, *14*, 353.

(16) (a) Suh, S. W.; Chen, J. W.; Motamedi, M.; Bell, B.; Listiak, K.; Pons, N. F.; Danscher, G.; Frederickson, C. J. *Brain Res.* **2000**, *852*, 268. (b) Choi, D. W.; Koh, J. Y. *Annu. Rev. Neurosci.* **1998**, *21*, 347.

(17) Cuajungco, M. P.; Lees, G. J. *Neurobiol. Dis.* **1997**, *4*, 137.

(18) Jiang, P.; Guo, Z. *Coord. Chem. Rev*. **2004**, *248*, 205.

(19) Frederickson, C. J.; Kasarskis, E. J.; Ringo, D.; Frederickson, R. E. *J. Neurosci. Methods* **1987**, *20*, 91.

(20) Taki, M.; Wolford, J. L.; O' Halloran, T. V. *J. Am. Chem. Soc.* **2004**, *126*, 712.

(21) Burdette, S. C.; Frederickson, C. J.; Bu, W.; Lippard, S. J. *J. Am. Chem. Soc.* **2003**, *125*, 1778.

(22) Chang, C. J.; Nolan, E. M.; Jaworski, J.; Okamoto, K.-I.; Hayashi, Y.; Sheng, M.; Lippard, S. J. *Inorg. Chem.* **2004**, *43*, 6774.

(23) Chang, C. J.; Nolan, E. M.; Jaworski, J.; Burdette, S. C.; Sheng, M.; Lippard, S. J. *Chem. Biol.* **2004**, *11*, 203.

(24) (a) Hirano, T.; Kikuchi, K.; Urano, Y.; Nagano, T. *J. Am. Chem. Soc.* **2002**, *124*, 6555 (b) Hirano, T.; Kikuchi, K.; Urano, Y.; Higuchi, T.; Nagano, T. *J. Am. Chem. Soc.* **2000**, *122*, 12399.

(25) Mahadevan, I. B.; Kimber, M. C.; Lincoln, S. F.; Tiekink, E. R. T.; Ward, A. D.; Betts, W. H.; Forbes, I. J.; Zalewski, P. D. *Aust. J. Chem.* **1996**, *49*, 561.

(26) Budde, T.; Minta, A.; White, J. A.; Kay, A. R. *Neuroscience* **1997**, *79*, 347.

(27) Shults, M. D.; Pearce, D. A.; Imperiali, B. *J. Am. Chem. Soc.* **2003**, *125*, 10591.

(28) Henary, M. M.; Fahrni, C. J. *J. Phys. Chem. A* **2002**, *106*, 5210.

Scheme 1

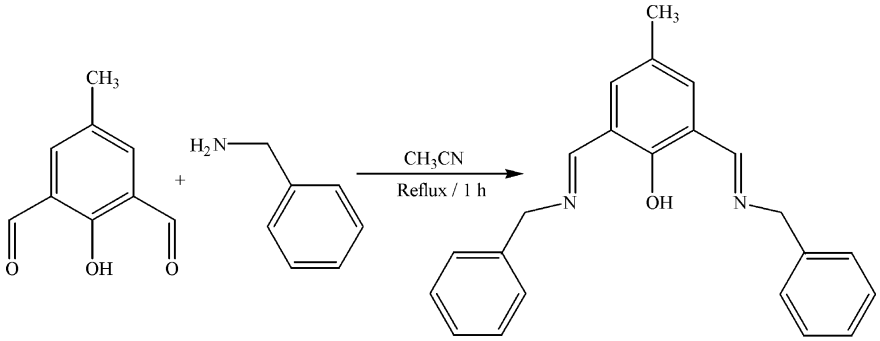

HL

Solvents used for spectroscopic studies were purified and dried by standard procedures before use.[29] FT-IR spectra were obtained on a Nicolet MAGNA-IR 750 spectrometer with samples prepared as KBr pellets. Elemental analysis was carried out in a 2400 Series-II CHN analyzer, Perkin-Elmer, Norwalk, CT. Absorption and luminescence spectra were studied on a Shimadzu UV2100 UV−vis recording spectrophotometer and a Perkin-Elmer LS 55 Luminescence Spectrometer, respectively. The ESI-MS was recorded on Qtof Micro YA263 mass spectrometer. Fluorescence life times were determined from time-resolved intensity decay by the method of time-correlated single-photon counting using a picosecond diode laser at 403 nm as light source.

Imaging System. The imaging system was comprised of an inverted fluorescence microscope (IX-70, Olympus, Tokyo, Japan), digital compact camera (Olympus, model C-5060), and an image processor (CAMEDIA Master, Olympus). The microscope was equipped with a halogen lamp, a mercury burner, and objective lens [×40 (B16F10 and A375)].

Preparation of Cells. A375 human melanoma and B16F10 mouse melanoma cells procured from National Center for Cell Science, Pune, India, were cultured in Dulbecco's modified Eagle's medium (DMEM, Gibco BRL) supplemented with 10% FBS (Gibco BRL) and 1% antibiotic mixture containing penicillin, streptomycin, and neomycin (PSN, Gibco BRL) at 37 °C in a humidified incubator with 5% CO_2. For experimental study, cells were grown to 80−90% confluence, harvested with 0.025% trypsin (Gibco BRL) and 0.52 mM EDTA (Gibco BRL) in PBS (phosphate-buffered saline, Sigma Diagnostics), plated in a six-well culture plate (NUNC, Roskilde, Germany) at a density of 5×10^5 cells/mL, and allowed to reequilibrate for 24 h before loading. Then the cells were rinsed with PBS and incubated with PBS containing 20 μM of **HL** for 30 min at 37 °C. The cells were then washed with PBS thrice and mounted on a microscope stage.

Synthesis of 4-Methyl-2,6-bis(((phenylmethyl)imino)methyl)-phenol (HL). The compound was prepared by a slight modification of the procedure described previously.[30] 4-Methyl-2,6-diformylphenol was synthesized starting from *p*-cresol by following a published procedure.[31] To a solution of 4-methyl-2,6-diformylphenol (0.328 g, 2 mmol) in 25 mL of acetonitrile was added phenylmethylamine (0.428 g, 4 mmol) in 10 mL of acetonitrile. The reaction mixture was refluxed for 1 h. The solution was filtered, concentrated on a rotaevaporator to dryness, and kept overnight at 4 °C. The resulting Schiff base, **HL** (4-methyl-2,6-bis(((phenylmethyl)imino)methyl)-phenol) (Scheme 1) is solid (yield = 0.58 g, 85%). Data for **HL** are as follow. Anal. Calcd for $C_{23}H_{22}N_2O$: C, 80.67; H, 6.48; N, 8.18. Found: C, 80.58; H, 6.42; N, 8.10. FT-IR (KBr phase) (ν/cm^{-1}): 1635, 1600. ^{1}H NMR (300 MHz, $CDCl_3$; δ): 2.30 (s, 3H, Ar−CH_3), 4.83 (s, 4H, CH), 7.26−7.40 (m, 12H, Ar−CH), 8.67 (s, 2H, HC═N). HRMS [(M + H$^+$)/*z*, (%)]: simulated for $C_{23}H_{23}N_2O$, 343.1797 (100); found, 343.0690 (100).

Synthesis of $[Zn_6(L)_2(OH)_2(CH_3COO)_8]$ (1). A 10 mL acetonitrile solution of zinc(II) acetate dihydrate (0.131 g, 0.6 mmol) was added slowly to a magnetically stirred 10 mL acetonitrile solution of the ligand (**HL**) (0.068 g, 0.2 mmol). The mixture was stirred in air for 30 min whereby a yellow solution was formed. It was filtered and kept in air. Pale yellow prismatic single crystals of **1** suitable for X-ray crystallography were obtained on slow evaporation of the filtrate at ambient temperature within 3 days (yield: 80%). Anal. Calcd for $C_{62}H_{68}N_4O_{20}Zn_6$: C, 47.09; H, 4.33; N, 3.54. Found: C, 47.11; H, 4.30; N, 3.48. FT-IR (KBr phase) (cm^{-1}): 3433 br, 3215 br, 1647 vs, 1556 vs, 1452 m, 1323 m, 1238 w, 1113 vs, 625 s, 489 w (br, broad; w, weak; m, medium; s, strong; vs, very strong).

X-ray Data Collection and Structure Determination. Crystal data of 1 are summarized in Table 1. The diffraction experiment was carried out on a Bruker SMART CCD area-detector diffractometer at 296 K. No crystal decay was observed, so that no time-decay correction was needed. The collected frames were processed with the software SAINT,[32] and an empirical absorption correction was applied (SADABS)[33] to the collected reflections. The calculations were performed using the Personal Structure Determination Package[34] and the physical constants tabulated therein.[35] The structure was solved by direct methods (SHELXS)[36] and refined by full-matrix least squares using all reflections and minimizing the function $\Sigma w(F_o^2 - kF_c^2)^2$ (refinement on F^2). All the non-hydrogen atoms were refined with anisotropic thermal factors. The 15 hydrogen atoms of the 5 CH_3 groups were refined with an isotropic thermal parameter. All the other hydrogen atoms were placed in their ideal positions (C−H or O−H = 0.97 Å), with the thermal parameter *U* 1.10 times that of the atom to which they are attached, and not refined. In the final Fourier map the maximum residual was 1.35(20) e Å^{-3} at 0.87 Å from Zn1.

CCDC 638646 contains the supplementary crystallographic data for this paper. These data can be obtained free of charge from the

(29) Perrin, D. D.; Armarego, W. L. F.; Perrin, D. R. *Purification of Laboratory Chemicals*; Pergamon Press: Oxford, U.K., 1980.
(30) Grzybowski, J. J.; Urbach, F. L. *Inorg. Chem.* **1980**, *19*, 2604.
(31) Gagne, R. R.; Spiro, C. L.; Smith, T. J.; Hamann, C. A.; Thies, W. R.; Schiemke, A. K. *J. Am. Chem. Soc.* **1981**, *103*, 4073.
(32) *SAINT Reference Manual*; Siemens Energy and Automation: Madison, WI, 1994−1996.
(33) Sheldrick, G. M. *SADABS, Empirical Absorption Correction Program*; University of Gottingen: Gottingen, Germany, 1997.
(34) Frenz, B. A. *Comput. Phys.* **1988**, *2*, 42.
(35) *Crystallographic Computing 5*; Oxford University Press: Oxford, U.K., 1991; Chapter 11, p 126.

Table 1. Crystallographic Data for **1**

formula	$C_{62}H_{68}N_4O_{20}Zn_6$
M	1581.47
color	pale yellow
cryst system	triclinic
space group	$P\bar{1}$
a/Å	10.740(1)
b/Å	12.927(1)
c/Å	13.281(1)
α/deg	115.06(1)
β/deg	96.34(1)
γ/deg	101.98(1)
V/Å^3	*1592.5(2)*
Z	*1*
F(000)	808
D_c/g cm^{-3}	1.649
T/K	296
λ(Mo Kα)/Å	0.710 73
cryst dimens/mm	0.21 × 0.35 × 0.36
μ(Mo Kα)/cm^{-1}	23.56
min and max transm factors	0.853−1.000
scan mode	w
frame width/deg	0.30
time frame^{-1}/s	20
no. of frames	2450
detector−sample dist/cm	6.00
θ-range/deg	3−27
reciprocal space explored	full sphere
no. of reflcns (tot., indpndt)	24 368, 8042
R_{int}	0.0185
final R_2 and R_{2w} indices[a] (F^2, all reflcns)	0.055, 0.084
conventional R_1 index [$I > 2\sigma(I)$]	0.034
reflcns with $I > 2\sigma(I)$	5818
no. of variables	475
goodness of fit[b]	1.065

[a] $R_2 = [\Sigma(|F_o^2 - kF_c^2|/\Sigma F_o^2]$, $R_{2w} = [\Sigma w/(F_o^2 - kF_c^2)^2/\Sigma w(F_o^2)^2]^{1/2}$. [b] $[\Sigma w(F_o^2 - kF_c^2)^2/(N_o - N_v)]^{1/2}$, where $w = 4F_o^2/\sigma(F_o^2)^2$, $\sigma(F_o^2) = [\sigma^2(F_o^2) + (pF_o^2)^2]^{1/2}$, N_o is the number of observations, N_v is the number of variables, and $p = 0.04$.

Cambridge Crystallographic Data Centre via www.ccdc.cam.ac.uk/data_request/cif.

Results and Discussion

Fluorescence Property. The emission spectrum of the sensor (**HL**) under physiological condition (100 mM HEPES buffer at pH 7.4) excited at 400 nm exhibits the emission maximum at 530 nm at 25 °C with a quantum yield of only 0.040. We measured the emission intensities of the sensor molecule in the presence of various concentrations of Zn^{2+} (0−1.0 mM concentration). The sensor showed changes in fluorescence intensity and a new peak appeared at 484 nm, retaining 530 nm as a shoulder as suggested by unsymmetrical shape of the emission spectrum (Figure 1), and the fluorescence quantum yield ($\Phi = 0.250$) increased more than 6-fold. The fluorophore and the guest binding units were covalently integrated to modulate the photophysical responses of the ligand, **HL**, by introducing a possible excited-state electron-transfer process between the two. The system shows selective chelation enhanced fluorescence (CHEF) in the presence of Zn^{2+} ion. The experiment reveals that there is a significant increase in fluorescence intensity for **1**. The new peak of emission band (484 nm) by the complex **1** as compared to that at 530 nm of the free ligand is quite

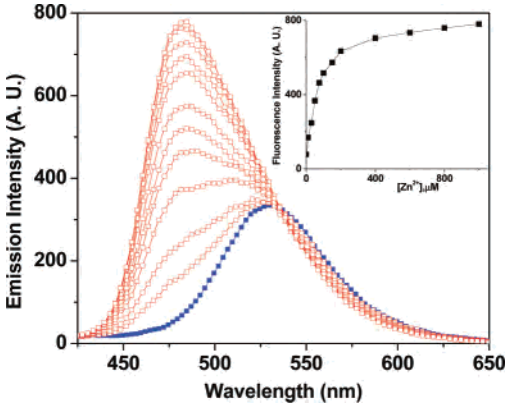

Figure 1. Emission spectra of 50 μM of **HL** in the presence of 0, 10, 30, 50, 75, 100, 150, 200, 400, 600, 800, and 1000 μM of free Zn^{2+} ions in 100 mM HEPES buffer at pH 7.4 at room temperature (excitation 400 nm, emission 530 nm). Inset: Fluorescence enhancement versus concentration of Zn^{2+}.

unexpected (Figure 1), as one would expect the emission band of the free ligand to be at higher energy related to that of the complex because of its relatively high-energy excitation band. This anomaly can be explained by the fact that excited states resulting from complexes of Zn^{2+} are typically ligand-centered (LC) in nature owing to the inability of the d^{10} metal center to participate in low-energy charge transfer for metal-centered transitions.[37] Therefore, the emission from $[Zn_6(L)_2(OH)_2(CH_3COO)_8]$ (**1**) is believed to arise from an excited-state centered on **HL** which contains a phenolic proton (Scheme 1). It is well-established that the emissive organic phenol, 4-methyl-2,6-diformylphenol, undergoes a blue shift of its own band (from 530 to 445 nm) upon treatment with a base B (e.g., piperidine or triethylamine), and this observation is believed to support the existence of an equilibrium between undissociated phenol and a proton-transferred species of phenol with the formation of phenoxide anion and BH^+ cation.[38] The same analogy can be extended to the present system because the phenolic proton of the ligand is deprotonated upon complexation with Zn^{2+}, and this proton should be transferred to the acetate anion of the precursor zinc(II) acetate dihydrate in the solution. We performed the emission experiment on the free ligand in the presence of an added base, e.g., triethylamine, in aqueous solution and found that, on addition of triethylamine, a new band appeared at around 458 nm. This indicates the existence of an equilibrium between an undissociated **HL** and a proton-transferred species of **HL** (see Supporting Information, Figure S1).

The electrospray mass spectrum of the complex **1** was obtained in aqueous solution. The spectrum shows peaks at *m*/*z* 1617.76 and 1322.73 that can be assigned to the $[Zn_6(L)_2(OH)_2(CH_3COO)_8]\cdot 2H_2O$ and $[Zn_4(L)_2(OH)_2(CH_3COO)_4(H_2O)_6]$ species, respectively. The isotopic distributions for the above molecular species obtained experimentally (see

(36) Sheldrick, G. M. *SHELXS 86. Program for the solution of crystal structures*; University of Gottingen: Gottingen, Germany, 1985.

(37) (a) Dollberg, C. L.; Turro, C. *Inorg. Chem.* **2001**, *40*, 2484. (b) Roundhill, D. M. *Photochemistry and Photophysics of Metal Complexes*; Fackler, J. P., Ed.; Modern Inorganic Chemistry Series; Plenum Press: New York, 1994; pp 56−57.

(38) (a) Mukherjee, S. *Indian J. Chem.* **1987**, *26A*, 1002. (b) Das, R.; Mitra, S.; Mukherjee, S. *Bull. Chem. Soc. Jpn.* **1993**, *66*, 2492.

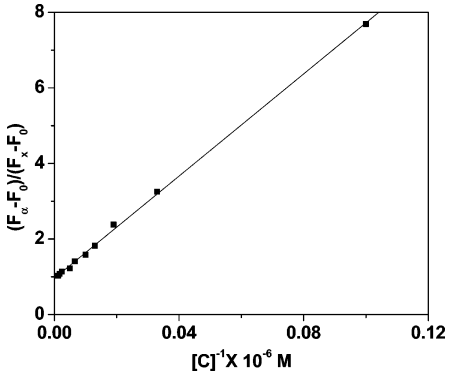

Figure 2. Binding constant, K (±15%), value determined from the slope of the plot as 1.5×10^4 M^{-1}.

Supporting Information, Figure S2) correspond to the simulated patterns. In this spectrum a peak at *m*/*z* 1617.76 assigned to $[Zn_6(L)_2(OH)_2(CH_3COO)_8]\cdot 2H_2O$ and a peak at *m*/*z* 1322.73 that corresponds to the $[Zn_4(L)_2(OH)_2(CH_3COO)_4(H_2O)_6]$ species corroborate the presence of the complex entity in solutions. Job's plot analysis revealed maximum emission at 1:3 ratio (**HL**:Zn^{2+}) (see Supporting Information, Figure S3). These data suggested that the complex species in solution should form 1:3 complex with Zn^{2+} which is clearly evident from the crystal structure of Zn^{2+}−ligand complex **1** (see later). To observe the binding interaction with Zn^{2+} in buffer medium, the binding constant value has been determined from the emission intensity data following the modified Benesi−Hildebrand equation:[39a,b] $1/\Delta F = 1/\Delta F_{max} + (1/K[C])(1/\Delta F_{max})$. Here $\Delta F = F_x - F_0$ and $\Delta F_{max} = F_\infty - F_0$, where F_0, F_x, and F_∞ are the emission intensities of **HL** considered in the absence of Zn^{2+}, at an intermediate Zn^{2+} concentration, and at a concentration of complete interaction, respectively, and where K is the binding constant and [C] the Zn^{2+} concentration. From the plot of $(F_\infty - F_0)/(F_x - F_0)$ against $[C]^{-1}$ for **HL** (Figure 2), the value of K (±15%) extracted from the slope is 1.5×10^4 M^{-1}. We also studied the effect of Zn^{2+} addition on the fluorescence decay behavior of **HL**. The fluorescence lifetime (τ) of **HL** in the working buffer medium is 2.09 ns. The results of fluorescence lifetime measurements (see Supporting Information, Figure S4) indicate that changes in lifetime would be associated with any number of possible mechanisms for fluorescence enhancement and not only PET (photoinduced electron transfer). The time-resolved spectrum appears to display at least two components. Since the mechanism of fluorescence enhancement is a change in rigidity upon binding of zinc ion, a different mechanism other than PET may be of significance. According to the equations[39c] $\tau^{-1} = k_r + k_{nr}$ and $k_r = \Phi_f/\tau$, the radiative rate constant k_r and total nonradiative rate constant k_{nr} of **HL** and **HL** binding with Zn^{2+} were calculated and listed in Table S1. The data suggest that k_{nr} has just slightly changed but the factor that induces fluorescent enhancement is mainly ascribed to the increase of k_r.

(39) (a) Mallick, A.; Chahattopadhyay, N. *Photochem. Photobiol.* **2005**, *81*, 419. (b) Benesi, H. A.; Hildebrand, J. H.; *J. Am. Chem. Soc.* **1949**, *71*, 2703. (c) Turro, N. J. *Modern Molecular Photochemistry*; Benjamin/Cummings Publishing Co., Inc.: Menlo Park, CA, 1978.

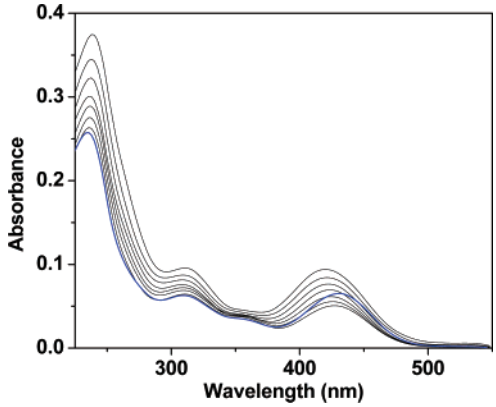

Figure 3. UV−vis spectral changes of **HL** upon addition of Zn^{2+} in 100 mM HEPES buffer at pH 7.4 at room temperature ([**HL**] = 50 μM, [Zn^{2+}] = 0, 10, 25, 50, 75, 100, 125, 150 μM).

Upon gradual addition of Zn^{2+} to a buffer solution of **HL**, the fluorescence intensity of the 530 nm band is meagerly changed along with the emergence of a new emission bend centered at 484 nm. It allows the ratiometric signaling when the ratio of the fluorescence output at two different wavelengths is plotted as a function of the concentration of Zn^{2+} (see Supporting Information, Figure S5). As can be seen, I_{484}/I_{530} increases with the concentration of Zn^{2+} ions in the range studied.

Absorption Study. The mode of coordination of **HL** with Zn^{2+} was investigated by spectrophotometric titration at 25 °C in 100 mM HEPES buffer (pH 7.4). Figure 3 illustrates a typical UV−vis titration curve of **HL** with added Zn^{2+}. As can be seen from Figure 3, the absorption intensity of **HL** at 234 nm gradually increases as the concentration of Zn^{2+} increases stepwise. Moreover, a new absorption peak appears at 418 nm in the UV−vis spectrum of the HL−Zn^{2+} system, and its intensity also gradually increases with the addition of Zn^{2+}. This absorption peak is likely to be due to the coordination of **HL** with Zn^{2+}.[40]

Metal Ion Competition Studies. To enable further understanding of this phenomenon, we have examined the effects of various metal ion additives on the spectral features of **HL**. Selectivity assays (Figure 4) were performed under physiological condition (100 mM HEPES buffer at pH 7.4) excited at 400 nm. Figure 4 illustrates the fluorescence intensities of **HL** (50×10^{-6} M) in presence of various metal ions. It is observed that, among the metal ions studied, only Zn^{2+} significantly modulates the fluorescence spectra of **HL**. Other cations which exist at high concentrations in living cells, e.g., Ca^{2+}, Mg^{2+}, Na^+, and K^+, do not enhance the fluorescence intensity even at a high concentration (150×10^{-6} M) as shown in Figure 4. These results are presumably due to the poor complexation of alkali metals or alkaline earth metals with the chelator (**HL**), on the basis of the absence of any obvious change of UV−visible spectrum upon addition of these cations. This also does not interfere with the Zn^{2+}-induced fluorescence enhancement. Emission spectrum of **HL** (50×10^{-6} M) was recorded upon addition

(40) Prabhakar, M.; Zacharias, P. S.; Das, S. K. *Inorg. Chem.* **2005**, *44*, 2585.

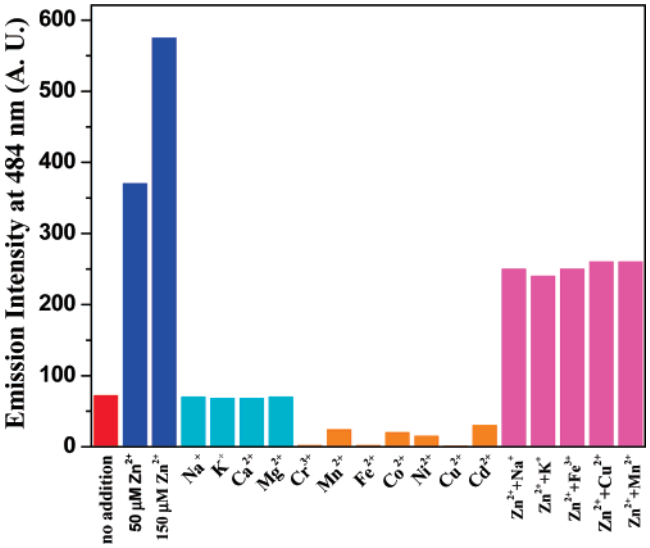

Figure 4. Relative fluorescence intensity change profile of **HL** (50 μM) in the presence of various cations in 100 mM HEPES buffer at pH 7.4 at room temperature (excitation 400 nm).

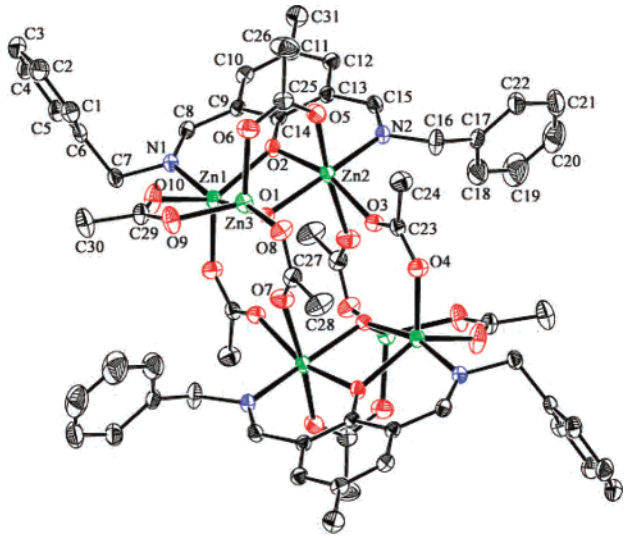

Figure 5. ORTEP drawing and atom numbering scheme for $[Zn_6(L)_2(OH)_2(CH_3COO)_8]$ (**1**). H atoms were omitted for clarity. The atoms are represented by 50% probability thermal ellipsoids.

of 3 equiv (150×10^{-6} M) of various heavy metal ions M (M = Mn^{2+}, Fe^{3+}, Cr^{3+}, Co^{2+}, Ni^{2+}, Cu^{2+}, Cd^{2+}). Among first-row transition metal cations, Cr, Mn, Fe, Co, Ni, and Cu quench the emission, owing to an electron or energy transfer between the metal cation and fluorophore known as the fluorescence quenching mechanism.[41] In the presence of 3 equiv of Cu^{2+}, Fe^{3+}, or Mn^{2+} together with Zn^{2+} (50×10^{-6} M), **HL** has almost no effect on the emission intensities. Cd^{2+} induces a slight enhancement of the emission intensity. However, Cd^{2+} is rarely present in biological systems and would not cause any problem in biological applications. The enhancement of fluorescence is attributed to the introduction of Zn^{2+} and the strong complexation occurs with **HL** evident from large binding constant value. The coordination of Zn(II) would impose rigidity and hence decrease the nonradiative decay of the excited state. Thus, Zn^{2+} can be distinguished from these heavy metal ions under physiological conditions.

(41) Sarkar, M.; Banthia, S.; Samanta, A. *Tetrahedron Lett.* **2006**, *47*, 7575.

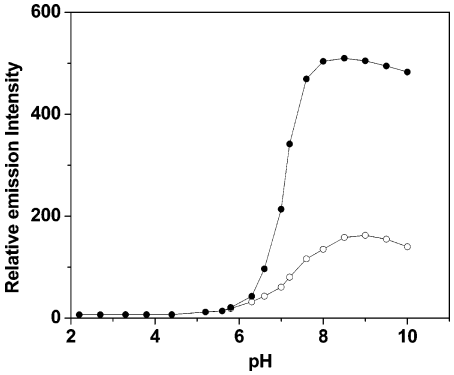

Figure 6. Fluorescence intensities of **HL** in the absence (open circles) and in the presence of Zn^{2+} (closed circles) at various pH values at room temperature (150 μM Zn^{2+} added to 50 μM of **HL**).

Table 2. Selected Bond Lengths (Å) and Bond Angles (deg)[a]

Zn1−O1	2.024(1)	Zn2−O5	2.118(2)
Zn1−O2	2.105(1)	Zn2−O7[a]	2.439(2)
Zn1−O4[a]	2.019(1)	Zn2−N2	2.020(1)
Zn1−O10	2.044(1)	Zn3−O1	1.949(1)
Zn1−N1	2.045(2)	Zn3−O6	1.956(2)
Zn2−O1	2.006(1)	Zn3−O8	1.935(2)
Zn2−O2	2.077(1)	Zn3−O9	1.958(2)
Zn2−O3	2.116(1)		
O1−Zn1−O2	78.00(5)	O1−Zn2−O5	96.34(5)
O1−Zn1−O10	94.72(7)	O2−Zn2−O5	95.26(7)
O2−Zn1−N1	86.53(5)	O1−Zn2−O7[a]	89.17(5)
O10−Zn1−N1	91.42(7)	O2−Zn2−O7[a]	86.28(6)
O1−Zn1−O4[a]	96.42(5)	O1−Zn3−O6	106.28(7)
O4[a]−Zn1−O10	104.85(8)	O1−Zn3−O8	121.71(6)
O1−Zn2−O2	79.06(5)	O1−Zn3−O9	108.24(7)
O1−Zn2−O3	88.65(5)	O6−Zn3−O8	103.27(8)
O2−Zn2−N2	90.66(7)	O6−Zn3−O9	105.43(9)
O3−Zn2−N3	99.22(6)	O8−Zn3−O9	110.58(8)

[a] Symmetry codes: (a) $1 - x$, $1 - y$, $1 - z$.

Crystal Structure of 1. Complex **1** crystallizes in the triclinic system, space group $P\bar{1}$ (No. 2) from acetonitrile solvent. A perspective view of $[Zn_6(\mathbf{L})_2(OH)_2(CH_3COO)_8]$ (**1**) with the atom-numbering scheme is shown in Figure 5. Selected bond lengths and bond angles are given in Table 2. This is a discrete hexanuclear complex. The asymmetric unit of complex **1** consists of three Zn^{2+}, one binucleating tridentate ligand (4-methyl-2,6-bis(((phenylmethyl)imino)-methyl)phenolate), one μ_3-hydroxide, and four acetate ions. Atom Zn1 is coordinated by a μ_2-phenoxo oxygen atom (O2) and N1 atom of the ligand **HL**, a μ_3-hydroxo oxygen atom (O1), and two μ_2-acetato oxygen atoms {O4[a] [(a) $1 - x$, $1 - y$, $1 - z$) and O10}. On the other hand, Zn2 is connected by the μ_2-phenoxo oxygen atom (O2) and N2 atom of the ligand, the same μ_3-hydroxo oxygen atom, and three μ_2-acetato oxygen atoms (O3, O5, and O7[a], "a" as above). As a consequence, Zn1 and Zn2 display coordination numbers 5 and 6, respectively, while Zn3 has the coordination number 4 and is linked by the same μ_3-hydroxo oxygen atom and three μ_2-acetato oxygen atoms (O6, O8, and O9). It is quite evident from the crystal structure that the three Zn^{2+} ions in the asymmetric unit have three different environments in their coordination spheres. Hexacoordinated Zn2 adopts a distorted

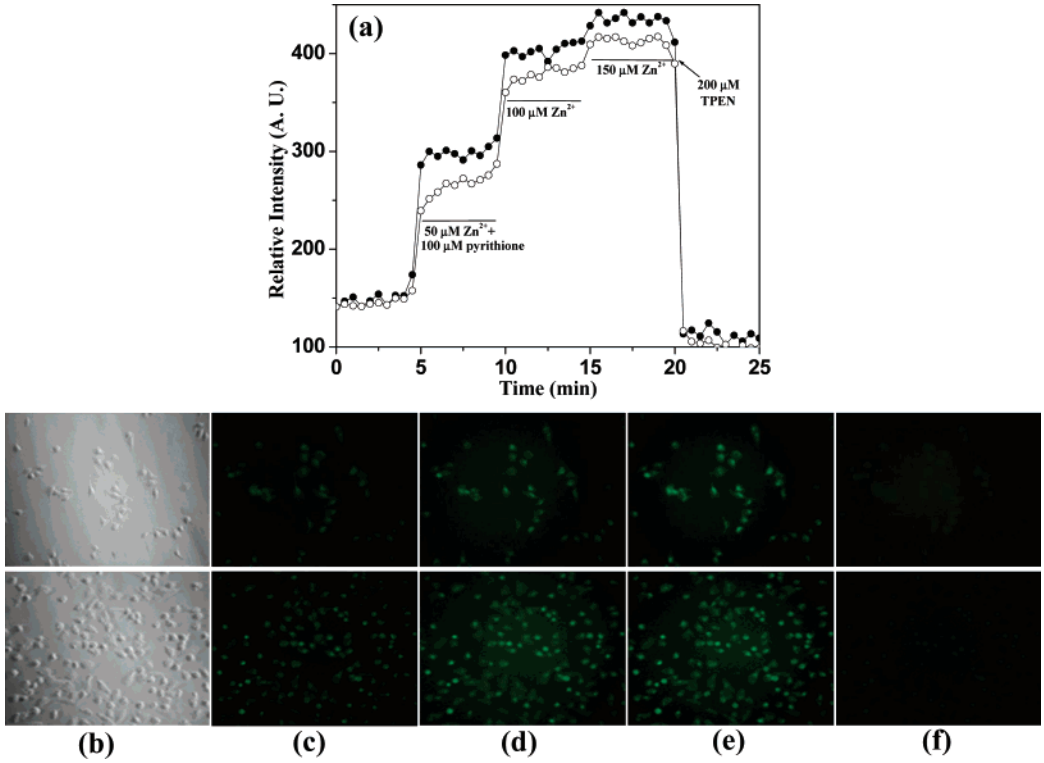

Figure 7. Phase contrast and fluorescence response of **HL** induced by intracellular Zn^{2+}. B16F10 and A375 cells incubated with 20 μM **HL** for 45 min at room temperature were washed with PBS, and fluorescence excited at 385−420 nm was measured at 30 s intervals. Cells were exposed to pyrithione (pyr, 100 μM) in the presence of sequentially increased concentration of added extracellular Zn^{2+} as indicated by (a) (closed circles for B16F10 and open circles for A375). Return of intracellular Zn^{2+} to the resting level was achieved by addition of TPEN (200 μM, indicated by the arrow). (b) Phase contrast image. (c−f) Fluorescence images incubated with **HL** (c, 2 min), with pyr and 50 μM Zn^{2+} (d, 7 min), with 150 μM Zn^{2+} (e, 17 min), and with 200 μM TPEN (f, 23 min). Top row: B16F10. Bottom row: A375.

octahedral geometry with cis angles ranging from 79.06(5) to 99.22(6)°. The pentacoordinated zinc atom (Zn1) is in a distorted square-pyramidal geometry, and the zinc ion is displaced by 0.502(1) Å from the best plane formed by atoms N1, O1, O2, and O10. The axial Zn1−O4^a [(a) $1 - x$, $1 - y$, $1 - z$) distance is 2.019(1).[42] Zn3 is in a distorted tetrahedral geometry with the bond angles ranging from 103.27(8) to 110.58(8)°.

Effect of pH. In addition to metal ion selectivity, we measured the fluorescence intensity of **HL** at various pH values in the presence and absence of Zn^{2+}. The fluorescence intensity of the **HL** decreases under acidic condition. This property arises from protonation of the phenolic hydroxyl group of the ligand, whose pK_a value has been determined to be 5.19.[43] Interestingly, **HL** showed good fluorescence sensing ability to Zn^{2+} over a wide range of pH values. As shown in Figure 6, **HL** shows no appreciable sensing ability to Zn^{2+} at a pH below 6.3, which may be due to the competition of H^+ below pH 6.3, but exhibits satisfactory Zn^{2+} sensing abilities when the pH is increased to the range 6.3−10. At pH ca. 7.4, the $F_{\mathbf{HL}/Zn(II)}/F_{\mathbf{HL}}$ reached its maximum value, indicating that **HL** possessed the highest sensing ability in an environment similar to serum (pH ca. 7.3). The pH sensitivity of the sensor is reflected by the drop of emission intensity by ca. 40% on going from pH 7.5 to 7.0. As the local pH can drop below 6.5 in many cell compartments and biofluids, the utility of this probe is restricted.

Cell Studies. We examined the application of **HL** to cultured living cells B16F10 mouse melanoma and A375 human melanoma by fluorescence microscopy (Figure 7). Since **HL** can be excited with a relatively long excitation wavelength, this compound is suitable for cellular application in comparison to the previously reported Zn^{2+}-selective luminescent sensors.[44] After incubation with 20 μM sensor, cells show weak fluorescence suggesting that the sensor molecule can be used intracellularly. We further examined whether the difference of affinity is reflected in the fluorescence microscopic imaging of intracellular Zn^{2+} or not. The intracellular concentration of Zn^{2+} was controlled with a Zn^{2+} ionophore, pyrithione (2-mercaptopyridine *N*-oxide), which brings the extracellular Zn^{2+} into the cytoplasm. We added various concentrations of Zn^{2+} with pyrithione, and the intracellular Zn^{2+} concentration was measured by fluorescence microscopy. With the increase of extracellular Zn^{2+} concentration, the fluorescence intensity of the compound increases. Figure 7 shows the fluorescence response of the sensor molecule. The fluorescence was measured at 30 s intervals for the different concentrations of zinc(II) acetate. The fluorescence intensity was saturated with 150 μM $Zn(OAc)_2$. Subsequent addition of the cell-permeable metal

(42) Yamami, M.; Furutachi, H.; Yokoyama, T.; Ōkawa, H. *Inorg. Chem.* **1998**, *37*, 6832.
(43) Albert, A.; Serjeant, E. P. *Determination of Ionization Constants. A Laboratary Manual*, 3rd ed.; Chapman and Hall: London, 1984.
(44) Hanaoka, K.; Kikuchi, K.; Kojima, H.; Urano, Y.; Nagano, T. *J. Am. Chem. Soc.* **2004**, *126*, 12470.

chelator *N*,*N*,*N*′,*N*′-tetrakis(2-pyridyl)ethylenediamine (TPEN) quenches the emission intensity consistent with the intracellular turn-on as a consequence of reversible zinc binding. These results suggested that **HL** can be used to monitor the changes of intracellular Zn^{2+} and should, therefore, be useful for clarifying the role of Zn^{2+} in biological processes in which the intracellular concentration of Zn^{2+} is important, for example, cell death induced by ischemia.[45]

Conclusion

We have investigated the zinc ion fluorescence sensing and binding properties of 4-methyl-2,6-bis(((phenylmethyl)-imino)methyl) phenol (**HL**), which displays high selectivity for Zn^{2+} and can be used as zinc ion-selective luminescent probe for biological application. The increase in emission in the presence of Zn^{2+} is accounted for by the formation of a metal−ligand complex (**1**). The X-ray crystal structure reveals that the **1** is a discrete hexanuclear complex, $[Zn_6(\mathbf{L})_2(OH)_2(CH_3COO)_8]$. An approximately 6-fold Zn^{2+}-selective chelation-enhanced fluorescence response in HEPES buffer (pH 7.4) is attributed to the strong coordination of Zn(II) that would impose rigidity and hence decrease the nonradiative decay of the excited state. It has been demonstrated that this system in HEPES buffer is highly selective over other various metal ions. By the incubation of cultured living cells (B16F10 mouse melanoma and A375 human melanoma) with **HL**, intracellular Zn^{2+} concentration could be monitored.

Acknowledgment. K.D. acknowledges the Council of Scientific and Industrial Research, New Delhi, India, for financial support. We appreciate the cooperation received from Professor Nitin Chattopadhyay, Department of Chemistry, Jadavpur University, Jadavpur, India.

Supporting Information Available: Emission spectra of **HL** and **HL** with added base triethylamine, ESI-MS of **1**, Job's plot, time-resolved fluorescence decay, Table S1, ratiometric signaling of fluorescence, and details of the crystallographic study (CIF). This material is available free of charge via the Internet at http://pubs.acs.org.

IC700420W

(45) Koh, J.-Y.; Suh, S. W.; Gwag, B. J.; He, Y. Y.; Hsu, C.Y.; Choi, D. W. *Science* **1996,** *272*, 1013.